scientific reports

Check for updates

OPEN

A single neuron subset governs a single coactive neuron circuit in *Hydra vulgaris*, representing a possible ancestral feature of neural evolution

Yukihiko Noro, Hiroshi Shimizu, Katsuhiko Mineta & Takashi Gojobori✉

The last common ancestor of Bilateria and Cnidaria is believed to be one of the first animals to develop a nervous system over 500 million years ago. Many of the genes involved in the neural function of the advanced nervous system in Bilateria are well conserved in Cnidaria. Thus, the cnidarian *Hydra vulgaris* is a good model organism for the study of the putative primitive nervous system in its last common ancestor. The diffuse nervous system of *Hydra* consists of several peptidergic neuron subsets. However, the specific functions of these subsets remain unclear. Using calcium imaging, here we show that the neuron subsets that express neuropeptide, Hym-176, function as motor circuits to evoke longitudinal contraction. We found that all neurons in a subset defined by the Hym-176 gene (*Hym-176A*) or its paralogs (*Hym-176B*) expression are excited simultaneously, followed by longitudinal contraction. This indicates not only that these neuron subsets have a motor function but also that a single molecularly defined neuron subset forms a single coactive circuit. This is in contrast with the bilaterian nervous system, where a single molecularly defined neuron subset harbors multiple coactive circuits, showing a mixture of neurons firing with different timings. Furthermore, we found that the two motor circuits, one expressing *Hym-176B* in the body column and the other expressing *Hym-176A* in the foot, are coordinately regulated to exert region-specific contraction. Our results demonstrate that one neuron subset is likely to form a monofunctional circuit as a minimum functional unit to build a more complex behavior in *Hydra*. This simple feature (one subset, one circuit, one function) found in *Hydra* may represent the simple ancestral condition of neural evolution.

The evolution of the nervous system in animals persists as one of the most intriguing and significant mysteries in modern biology. Recent molecular phylogenetic studies indicate that there are two conflicting scenarios as to when the first nervous system evolved; it evolved either before Ctenophora was diverged from the rest of metazoans[1,2] or after Porifera was diverged from them[3,4], depending on the controversial phylogenetic position of Ctenophora. In either case, however, since the cnidarian/bilaterian nervous system differs a lot from the ctenophore's one[5] and some nerve-less phyla (Placozoa and Porifera) evolved after Ctenophora, the ctenophore's nervous system might evolve independently from the cnidarian/bilaterian one. Thus, one of the first nervous systems probably evolved in the last common ancestor of Cnidaria and Bilateria over 500 million years ago. Despite these millions of years of divergence, an almost complete set of the neural genes needed to build the advanced nervous system in bilaterians is well conserved in cnidarians[6]. Therefore, the cnidarian *Hydra* is a good model organism for the study of the primitive nervous system and how it has evolved into the advanced one.

The nervous system of *Hydra* is a net-like structure extending throughout the body and consists of multiple subsets of neurons. All subsets that have been studied so far are peptidergic (Supplementary Fig. S1). There are at least four neuropeptides, GLWa[7], Hym-355[8], RFa[9] and Hym-176[10,11], present in the *Hydra* nerve net. The genes for GLWa and Hym-355 are co-expressed in the same neurons, which are scattered in the ectodermal layer all over the body. However, in the hypostome, there are some GLWa-positive and Hym-355-negative neurons together with the double-positive neurons[12,13]. RFa (*PreproA*)-expressing neurons are found in the tentacle,

Computational Biosciences Research Center, King Abdullah University of Science and Technology, Thuwal 23955-6900, Kingdom of Saudi Arabia. ✉email: takashi.gojobori@kaust.edu.sa

the hypostome, the upper body column, and the peduncle. The Hym-176 gene (*Hym-176A*) is expressed in the neurons of the hypostome, the body column, and the peduncle. *PreproA* and *Hym-176A* are only co-expressed in the peduncle neurons[10,12]. Neither RFa-expressing nor Hym-176-expressing neurons are overlapped with GLWa/Hym-355 double-positive neurons[12,13].

In addition to these observations, we recently demonstrated that the four-gene paralogs of *Hym-176A* are expressed in neurons in the tentacle (*Hym-176E*), the body column (*Hym-176B*), and the peduncle (*Hym-176C* and *Hym-176D*)[14]. *Hym-176B, Hym-176C,* and *Hym-176D* are all co-expressed with *Hym-176A*. Therefore, as summarized in Supplementary Fig. S1, there are at least seven mutually exclusive molecularly defined neuron subsets (classical subsets) in the ectodermal layer in *Hydra* (subset I; *GLWa/Hym-355*, subset II; *prepro A/C*, subset III; *prepro A/B*, subset IV; *Hym-176A/B*, subset V; *Hym-176A/C/D/prepro A*, subset VI; *Hym-176A/C/prepro A*, subset VII; *Hym-176E*). Furthermore, a recent single-cell RNA-seq study of *Hydra*[15] revealed a more precise molecular definition of nine neuron subsets (new subsets) in the ectodermal layer: subset I is further divided into subset ec3A, ec3B, and ec3C; subset III is further divided into subset ec4A and ec4B; both subsets V and VI form one single subset ec5; and the remaining subsets II/IV/VII correspond to subset ec2/ec1A/ec1B, respectively (Supplementary Fig. S1).

Despite the comprehensive anatomical features of the *Hydra* nervous system, the function of the neuron subset is entirely unknown. The three neuron subsets (ec1A, ec1B, and ec5) expressing *Hym-176A* and its paralogs (*Hym-176B, C, D, E*) cover the whole body of the animal in a region-specific manner (ec1A in body, ec1B in the tentacle, and ec5 in the peduncle), suggesting that these neuron subsets are related to region-specific functions. Therefore, here we focus on these neuron subsets and examine their localized function by raising transgenic *Hydra* expressing the calcium indicator, GCaMP6s[16], in each neuron subset.

Results

Functional characterization of neuron subsets expressing neuropeptide Hym-176 gene and its paralogs. We raised transgenic *Hydra* expressing the calcium indicator, GCaMP6s, in the neurons expressing each one of the *Hym-176* gene paralogs (*Hym-176A, B, C,* and *D*) under the control of the gene regulatory regions of these paralogs, as described previously[14]. The transgenic line, Hym-176B::GCaMP, visualized subset IV (ec1A) in the body column (Supplementary Fig. S1). The transgenic line, Hym-176A::GCaMP, Hym-176C::GCaMP, and Hym-176D::GCaMP, all visualized the same subset, i.e., subset V and VI (ec5) in the peduncle. We were unable to visualize subset VII (ec1B) in the tentacle due to the difficulty in generating the transgenic line, Hym-176E::GCaMP.

These subset-specific GCaMP6s expressions showed clear excitation patterns in each neuron subset (Movie 1–4). The shape of the blinking neurons and their resulting net-like structure were especially visible in the close-up view (Movie 5). We quantified the timing and the intensity of the excitation visible in the recorded movies. For example, we selected 18 neurons from the *Hym-176A*-expressing subset (ec5) in Movie 6 (Fig. 1A); their excitation patterns for 15 s are shown (Fig. 1B, Supplementary Fig. S2A). Each of the 18 neurons fired simultaneously at 2.22, 4.79, 6.81, 9.38, and 12.50 s (vertical dotted lines). The simultaneous firings in this subset (ec5) and the other subset (ec1A) were also visualized by the transgenic lines, Hym-176C::GCaMP (Fig. 1E,F, Supplementary Fig. S2C, Movie 8), Hym-176D::GCaMP (Fig. 1G,H, Supplementary Fig. S2D, Movie 9) for ec5, and Hym-176B::GCaMP for ec1A (Fig. 1C,D, Supplementary Fig. S2B, Movie 7). This simultaneous firing was confirmed by the distribution of the spike timing between all the tested neurons (Fig. 2B,E,H,I). For more than 80% of spikes (22/27), the spike timing of the tested neurons in the IQR (interquartile range) varied by less than 0.06 s. The neurons in the bud were all excited at the same time but different from those in the parental polyp (cell# 41,42, 45, 46, 49, and 54 in Fig. 1F, Supplementary Fig. S2C). These results suggest that each of the two neuron subsets (ec1A and ec5) forms a single coactive circuit and that the circuit in the bud at this developmental stage is independently regulated from the circuit in the parental polyp.

Although the timing of the firing was the same between neurons in a subset, the intensity of the firing and its time course profile varied between the neurons, e.g., high (cell #19, #24) or low intensity (cell #3, #10), and steady (cell #12, #18) or decaying (cell #4, #5, #23, #24) or atypical (cell #14) oscillation in the *Hym-176A*-expressing neuron subset, ec5 (Fig. 1B, Supplementary Fig. S2A). We observed these differential excitation profiles in the same subset with different transgenic lines (Fig. 1F,H, Supplementary Fig. S2C,D) and also in the different subset, ec1A (Fig. 1D, Supplementary Fig. S2B). These results indicate that neurons in a coactive circuit respond synchronously but differentially.

Quantitative analysis also demonstrated that the simultaneous excitation of neurons in each of the two subsets, ec1A and ec5, was well correlated with or was mostly followed by the longitudinal contraction. We evaluated the contraction by measuring the distance between the two designated neurons, usually the uppermost and the lowermost neuron in each subset (blue lines in Fig. 2A,D,G,J). Second-order differences in the distance (red lines in Fig. 2A,D,G,J) indicate a contraction status, i.e., fully relaxed at the local minimum and completely shrunk at the local maximum. Thus, fully relaxed at the local minimum indicates the start of contraction (vertical dashed red line in Fig. 2A,D,G,J). Cross-correlation between the representative neuron excitation (green line in Fig. 2A,D,G,J) and the second-order difference of the distance was above the 95% confidence interval cut-off (horizontal dashed blue line in Fig. 2C,F,I,L). Most (24 out of 27) of the neural excitations (vertical dashed black lines) were followed by longitudinal contractions (vertical dashed red lines) in less than 0.4 s (Fig. 2A,D,G,J). This delay between spike and contraction was far beyond the dispersion of spike timing among all tested neurons (median IQR: 0.06 s). For instance, for more than 74% (20/27) of spikes, contraction started later than Q3 (3-quantile) + 1.5 × IQR. For more than 51% (14/27) of spikes, contraction started later than Q3 + 3 × IQR (Fig. 2B,E,H,K). These results suggest that the dispersion of spike timing is minimal (almost at the same time) among the tested neurons in a subset, compared to the timing of the start of the contraction,

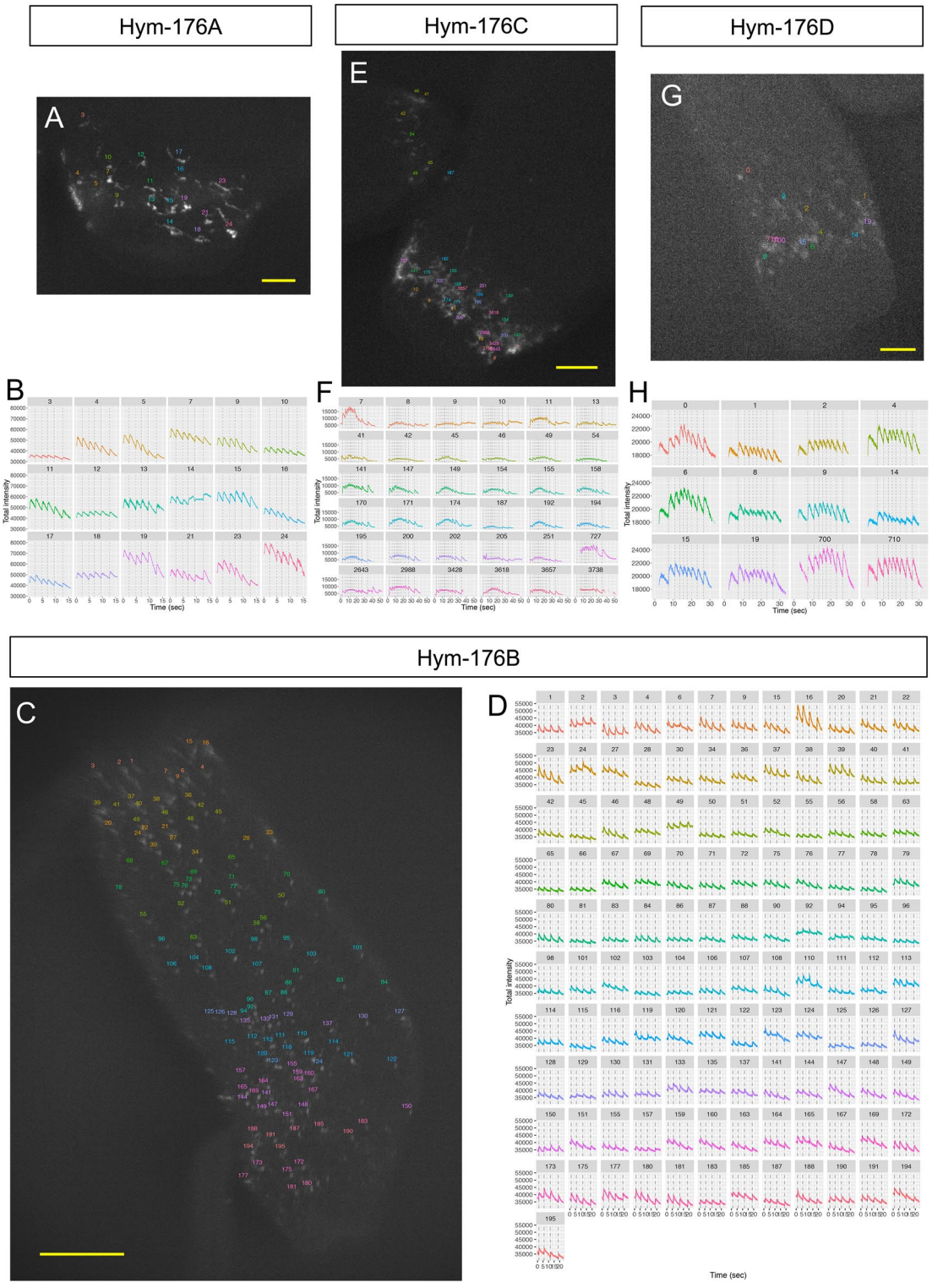

Figure 1. Simultaneous neuronal excitation of the peptidergic neuron subsets expressing neuropeptide gene *Hym-176* paralogs. *Hym-176A*-expressing neuron subset (**A,B**). *Hym-176B*-expressing neuron subset (**C,D**). *Hym-176C*-expressing neuron subset (**E,F**). *Hym-176D*-expressing neuron subset (**G,H**). Position of tested neurons (**A,C,E,G**). Neuronal activity (total intensity of GCaMP) is shown, with the vertical dashed lines indicating the average starting time of excitation of all tested neurons in each subset (B: 2.22, 4.79, 6.81, 9.38, 12.50 s; D: 1.09, 5.75, 11.72, 18.59 s; F: 2.13, 5.57, 7.98, 9.72, 11.60, 13.00, 14.83, 16.94, 19.45, 22.27, 26.26, 33.86 s; H: 7.37, 10.70, 13.37, 15.32, 17.41, 19.77, 22.80, 26.15 s) except neuron #41–54 in F (see text). The number in the strip and the color of the excitation profile for each subset correspond to cells in each one of A, C, E and G. Bar: 30 μm in A, 200 μm in C, 100 μm in E and 50 μm in G.

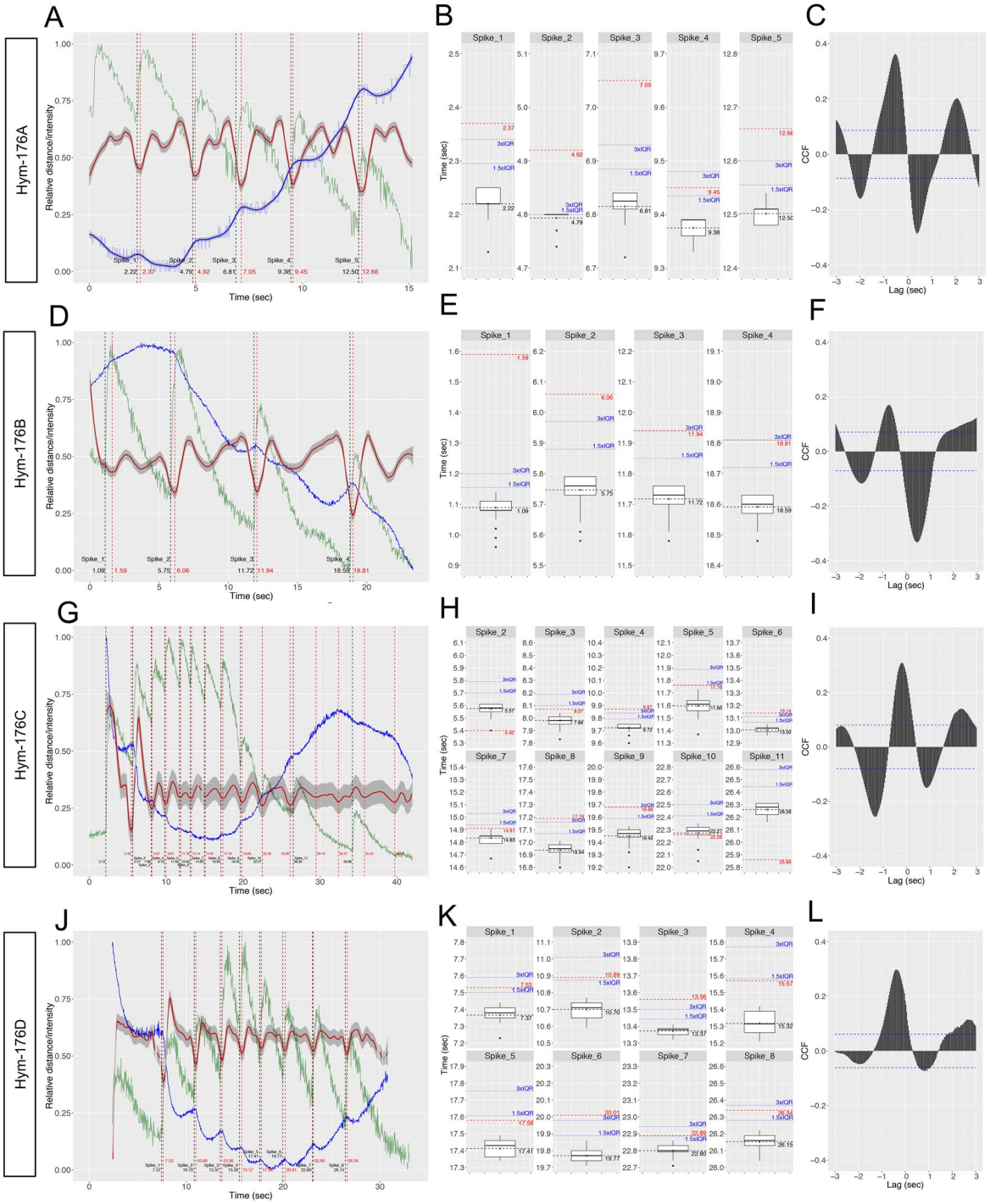

Figure 2. Neuronal activity in the Hym-176 peptidergic neuron subsets is associated with longitudinal contraction. *Hym-176A*-expressing neuron subsets (**A**–**C**). *Hym-176B*-expressing neuron subsets (**D**–**F**). *Hym-176C*-expressing neuron subsets (**G**–**I**). *Hym-176D*-expressing neuron subsets (**J**–**L**). Representative neuronal excitation in green; cell #24 in Fig. 1B (**A**), cell #16 in Fig. 1D (**D**), cell #7 in Fig. 1F (**G**) and cell #0 in Fig. 1H (**J**). Vertical dashed black lines show the spike train (**A,D,G,J**), as shown in Fig. 1B,D,F,H, respectively. Change in the distance between the two designated neurons in each subset is shown in blue (**A,D,G,J**); cell #14 and #17 in A, cell #3 and #150 in D, cell #13 and #149 in G, cell #0 and #8 in J. Second-order differences of the distance in red with 95% confidence interval (gray). Starting points of contraction (vertical red dashed line; A: 2.37, 4.92, 7.05, 9.45, 12.66 s; D: 1.59, 6.06, 11.94, 18.81 s; G: 5.40, 8.07, 9.87, 11.76, 13.14, 14.91, 17.19, 19.68, 22.26, 25.86 s; J: 7.53, 10.89, 13.56, 15.57, 17.58, 20.01, 22.89, 26.34 s). Box plot of the spike timing of all tested neurons for each spike (B, E, H, and K). The horizontal dashed black line indicates average spike timing, corresponding to the vertical dashed black line in (**A,D,G,J**). The horizontal dashed red line indicates the start of contraction, corresponding to the vertical dashed red line in (**A,D,G,J**). The horizontal dotted blue line indicates Q3 (3-quantile) + 1.5/3.0 × IQR (interquartile range). Cross-correlation (**C,F,I,L**) between representative neuronal excitation (solid green line) and longitudinal contraction (solid red line) in A, D, G, and J, respectively. The horizontal dashed blue line indicates the 95% confidence interval cut-off.

and that contraction indeed followed the preceding simultaneous excitation. These results demonstrate that the neuron subsets, ec1A and ec5 expressing the *Hym-176* gene paralogs, function as coactive motor circuits that evoke longitudinal contraction.

Besides those contractions associated with the preceding simultaneous excitation, we found some of the contractions were not associated with excitation (e.g., the contractions at 29.19, 32.07, 35.43, and 39.33 s in Fig. 2G). We do not yet entirely understand these unassociated contractions, but they may result from responses to the residual neurotransmitter released by the preceding contraction-associated excitation because they were mostly observed only after a series of the associated excitation. The contraction-unassociated excitation at 33.86 s in Fig. 2G may not have been able to evoke contraction due to epitheliomuscular desensitization of the neuronal excitation.

Two independent motor circuits coordinately function to regulate their region-specific contractions. Since both of the two coactive motor circuits, ec1A in the body column and ec5 in the peduncle, evoked longitudinal contraction, we examined whether these two circuits form a single coactive circuit or they function independently. At the onset of the quick and continuous longitudinal contraction (contraction burst[17,18]) in a double transgenic line or an operative chimera of single transgenic lines, we found that all the tested neurons in the peduncle (foot) neuron circuit only were simultaneously excited at their first spike (cell #13–#19 at 0 s in Fig. 3A,B, Supplementary Fig. S3A, Movie 10, cell #19–#89 at 6.42 s in Fig. 3C,D, Supplementary Fig. S3B, Movie 11). In contrast, those in the body neuron circuit were mostly silent, except for only a few neurons (cell #1 and #6 in Fig. 3D). This suggests that the two circuits were independently regulated without forming a single coactive circuit. Furthermore, with the spike only found in the foot circuit, 2–4 times stronger contraction of the foot than the body column was evoked (green arrows, at 0 s in Fig. 4A and 6.5 s in Fig. 4C). This indicated that the foot motor circuit was excited independently of the body motor circuit and evoked mostly foot contraction, at least at the onset of contraction burst. Subsequent contractions were synchronized again between the two circuits, following their synchronized excitation (Fig. 4C). However, sometimes subsequent contractions were anti-synchronized, especially when the foot was attached to the substrate, where it seemed like the foot tried to contract in vain because the body contraction simultaneously hampered it (Fig. 4A). These repelling contractions also indicate the independent motor function of these two circuits.

Although only the foot circuit was excited at the onset of contraction burst, the subsequent excitations were completely synchronized between the body and the foot circuits. We found that procaine, a voltage-gated sodium channel blocker, uncoupled the synchronized firing of these two circuits. The double transgenic line or the operative chimera of single transgenic lines treated with 1% procaine stopped contraction but maintained excitation. We observed a phase shift between the two coactive circuits: body one (blue) first and foot one (red) next (Figs. 3E–H, 4E–H, Supplementary Fig. S3C,D, Movies 12, 13), although sometimes foot one at 17.16 s preceded the body one at 17.28 s (spike_4 in Fig. 3G,H). These inter-circuit phase shifts (0.435 s on average for Fig. 4E,F and 0.262 s on average for Fig. 4G,H) were significantly larger than the intra-circuit dispersion of spike timing (0.087 s and 0.038 s on average, respectively). These shifts were not observed in the absence of procaine (Fig. 4B,D). We also found an irregular spike in the body neuron circuit at 16.31 s (Fig. 4G). All these results suggest that the two coactive motor circuits are not a single coactive circuit regardless of their inter-circuit synchronous firing that results from well-coordinated regulation of the two circuits.

Light-activated signaling center and unidirectional neurotransmission in the body neuron circuit. Besides the inter-circuit phase shift described above, we found that the prolonged procaine treatment also shifted the intra-circuit phase of excitation. For each of the four spikes, when we plotted the spike timing of all the tested neurons in the body circuit against the position of the neurons along the body axis, numbered in order beginning from head to foot, the cells closer to the lower end of the body column (in pink) were then excited later than the cells below the head (in blue) (Fig. 5A–C). This suggested that the wave of excitation transmitted unidirectionally from just below the head down to the foot (Movie 14). This unidirectional neurotransmission was probably too quick to be detected without the procaine, which slowed down the transmission.

Although the body neuron circuit is a single coactive motor circuit, as we mentioned above, we found that a group of neurons in the tentacle base and around the neck was excited earlier than the rest of the neurons in the circuit at the onset of the body contraction (Fig. 5D, Movie 15). This preceding excitation occurred more easily with more intense (off-filtered) blue light for the excitation of GCaMP (Fig. 5E), suggesting these neurons responded to light as a part of a light-sensing system to trigger the excitation of the motor circuit and subsequent longitudinal contraction. We believe these neurons belong to a subset different from the subset ec1A because detecting light or mediating the light-sensing requires an additional gene expression.

Taken together, the light-activated neurons near the head function as a signaling center to integrate light stimulation, and the body neuron circuit transfers the signal unidirectionally down to the foot.

Discussion

Before the calcium imaging technique became widely available, functional analysis of the nervous system in *Hydra* was quite limited, except for a series of pioneering studies by Josephson and Passano[17,18], who used intracellular electrical recordings. They showed that there are two types of action potentials in *Hydra*: one type is correlated with movement (e.g., contraction burst (CB) and tentacle pulse) while the other type is not correlated with movement (e.g., rhythmic potential (RP)). In their first successful attempt at calcium imaging of the *Hydra* nervous system, Dupre and Yuste functionally identified almost all of the neurons in *Hydra*. They categorized them into five coactive circuits, some of which seemed to correspond to the aforementioned action potentials.

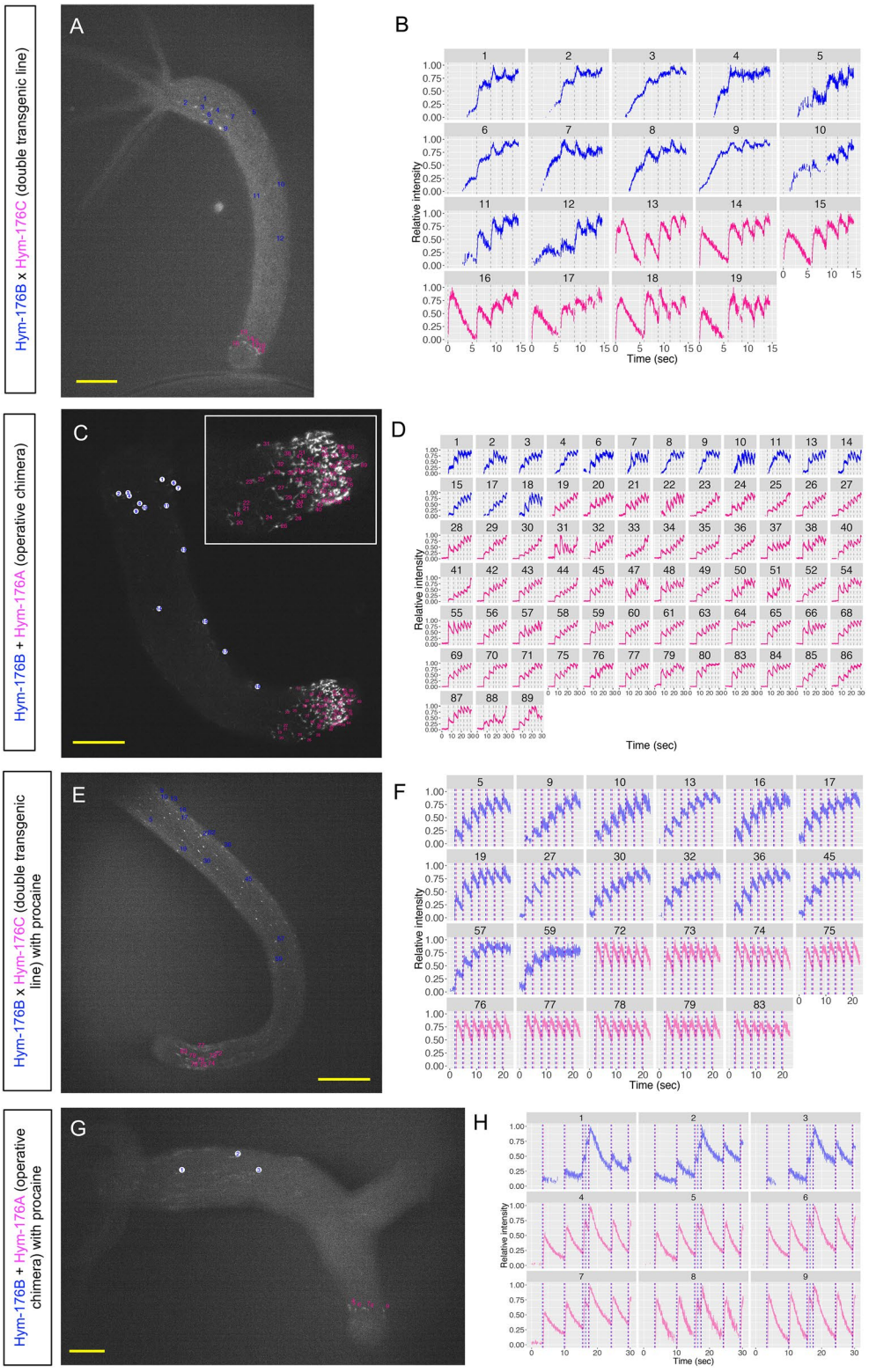

Figure 3. Simultaneously visualized neuronal activity of body and foot circuit. Double transgenic line of Hym-176B::GCaMP and Hym-176C::GCaMP with (**E,F**) or without (**A,B**) procaine treatment. The operative chimera of Hym-176B::GCaMP and Hym-176A::GCaMP with (**G,H**) or without (**C,D**) procaine treatment. Position of tested neurons (**A,C,E,G**). Neuronal activity (normalized intensity of GCaMP) with vertical dashed black lines indicating coactive neuronal excitation of both circuits ((**B**) 0, 5.84, 8.71, 11.11, 13.19 s; (**D**) 6.42, 11.99, 16.28, 19.08, 22.31, 25.61, 28.85 s). Neuronal activity (normalized intensity of GCaMP) with vertical dashed lines indicating coactive body neuron excitation in blue ((**F**) 1.94, 4.74, 7.94, 10.66, 13.32, 16.40, 19.42 s; (**H**) 3.25, 9.84, 15.30, 16.31, 17.28, 23.92, 29.00 s) and coactive foot neuron excitation in red ((**F**) 2.39, 5.16, 8.42, 11.11, 13.79, 16.78, 19.81 s; (**H**) 3.53, 10.09, 15.65, 17.16, 24.13, 29.21 s). The number in the strip and the color of the excitation profile for each animal correspond to cells in each one of (**A,C,E,G**) (body neuron circuit in blue and foot neuron circuit in red). Bar: 100 μm in (**A,E,G**) and 200 μm in (**C**).

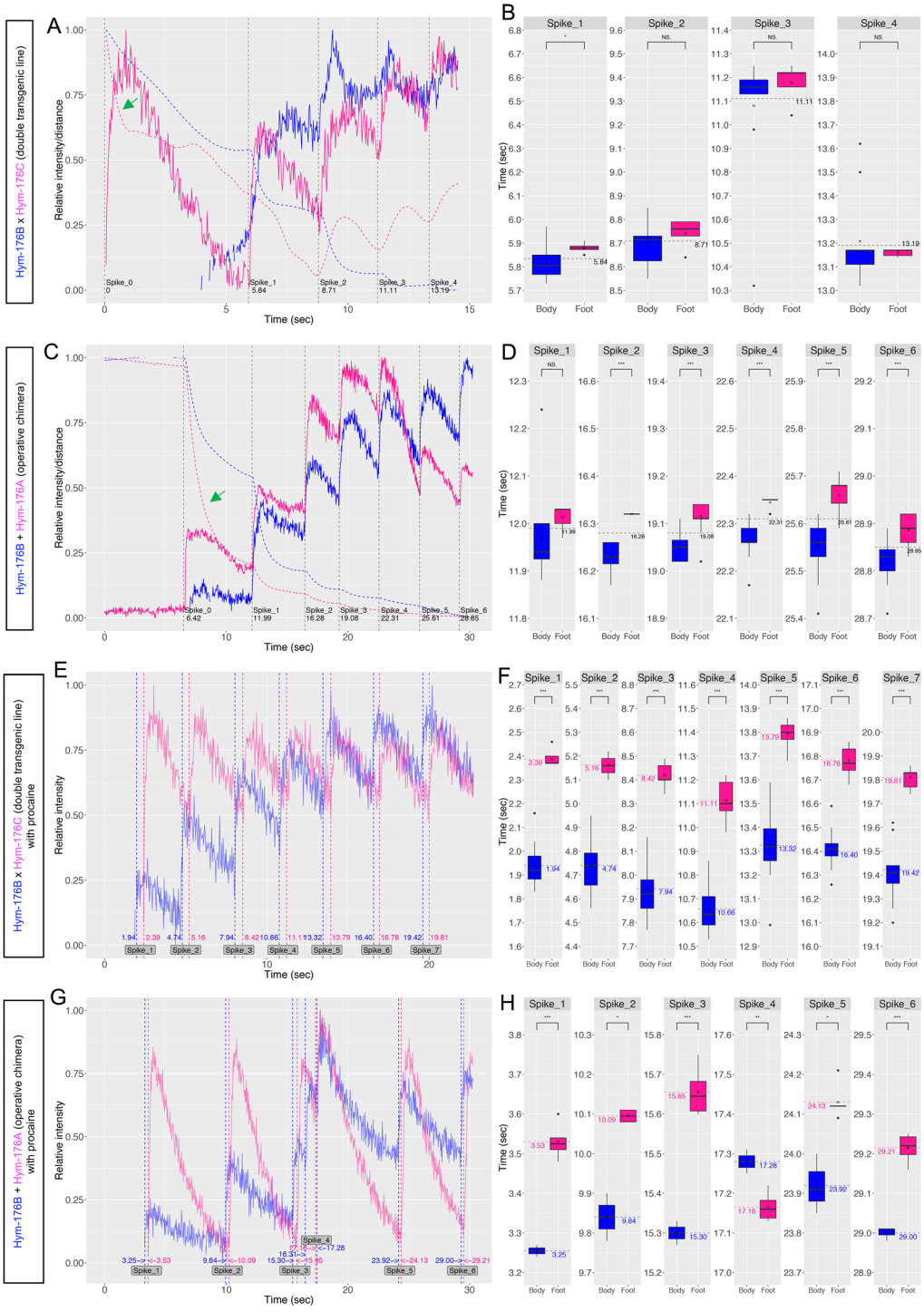

Figure 4. Coordinated interaction between body and foot neuronal circuit. Double transgenic line of Hym-176B::GCaMP and Hym-176C::GCaMP with (**E,F**) or without (**A,B**) procaine treatment. The operative chimera of Hym-176B::GCaMP and Hym-176A::GCaMP with (**G,H**) or without (**C,D**) procaine treatment. Normalized neuronal activity of representative neurons from body circuit in blue and foot circuit in red; cell #1 and #16 in Fig. 3B (**A**), cell #15 and #89 in Fig. 3D (**C**), cell #5 and #83 in Fig. 3F (**E**), cell #2 and #9 in Fig. 3H (**G**). Vertical dashed black/blue/red lines are as described in Fig. 3. Normalized distance between the three designated neurons in each animal was calculated for cell #9, #14 and #16 in Fig. 3B (**A**), and cell #7, #21 and #87 in Fig. 3D (**C**). Normalized distance between the first two neurons, shown by the dashed blue line, and between the last two neurons, shown by the dashed red line, indicates body and foot length, respectively. Box plot of the spike timing of all tested neurons in the body (blue) and foot (red) circuit for each spike (**B,D,F,H**). The horizontal dashed black line in (**B,D**) indicates the average spike timing of all tested neurons in both circuits, corresponding to the vertical dashed black line in (**A,C**), respectively. The horizontal dashed blue/red line in F and H indicates the average spike timing of all tested neurons in the body/foot circuit, corresponding to the vertical dashed blue/red line in (**E,G**), respectively. Statistical significance of the difference between average spike timings of body and foot circuit was evaluated by two-sided Student's t-test; NS: no significant difference; *$p < 0.05$; **$p < 0.01$; ***$p < 0.001$.

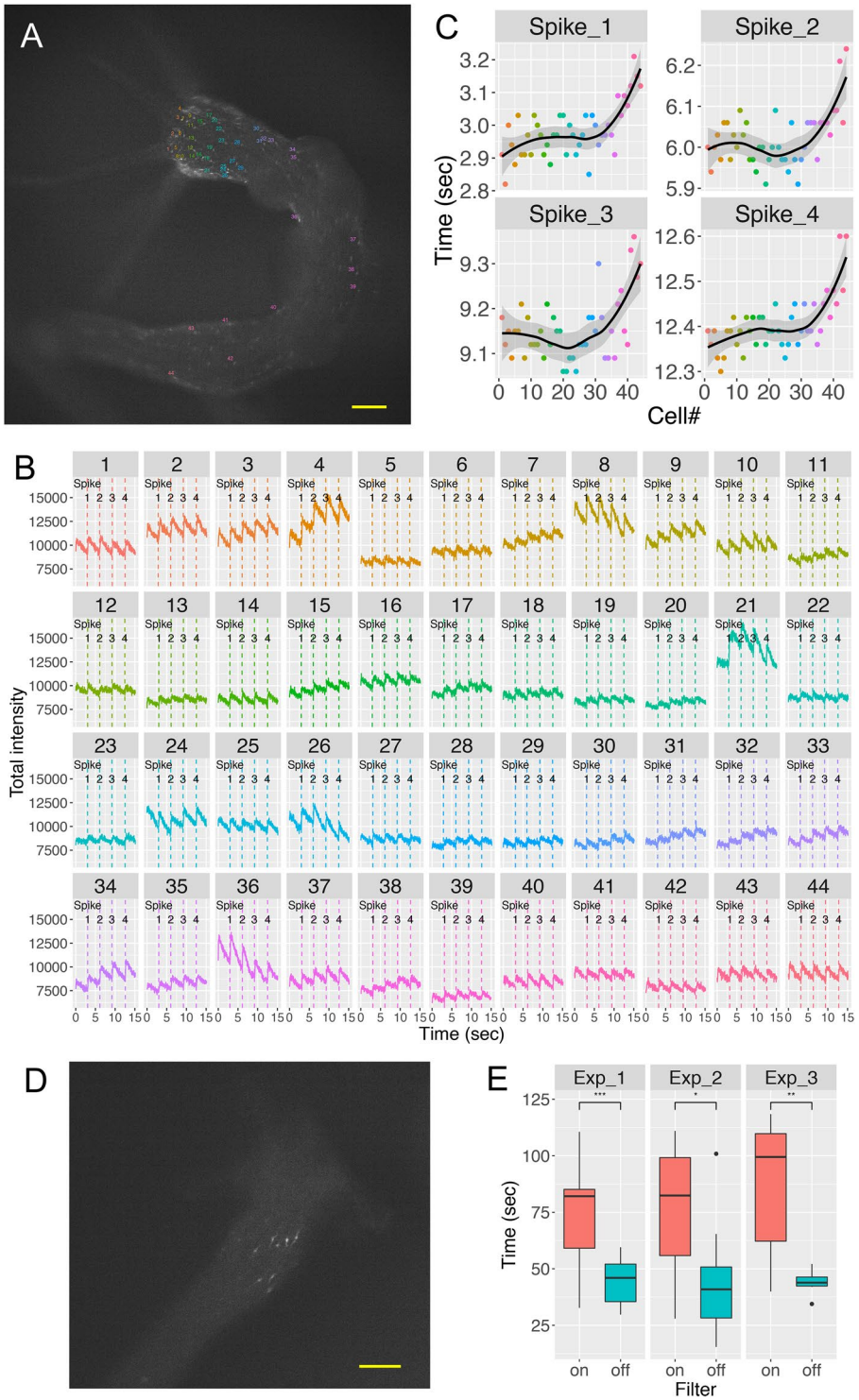

Figure 5. Unidirectional signal transmission in the body neuron circuit. Hym-176B::GCaMP transgenic animal was treated with procaine. Tested neurons are numbered according to their position, ascending from head to foot (cell#) (**A**). Neuronal activity (total intensity of GCaMP) with vertical lines indicating individual excitation spikes of each neuron (**B**). For each spike, the starting time is plotted against the cell# (**C**). The number in each strip, the color of the excitation profile in B, and the color of dots in C correspond to cells in A. The solid black line indicates loess regression with the 95% confidence interval in gray. Light-activated neurons in Hym-176B::GCaMP transgenic animal (**D**). Bar: 100 µm both in A and D. Box plot of time, which was taken by light-activated neurons to start excitation when exposed to blue light with or without dark filter (**E**). Three independent experiments were conducted (n = 22 for exp_1 and 2, and n = 14 for exp_3). Statistical significance of the difference between the average time to the beginning of excitation with and without a dark filter was evaluated using two-sided Student's t-test; NS: no significant difference; *$p < 0.05$; **$p < 0.01$; ***$p < 0.001$.

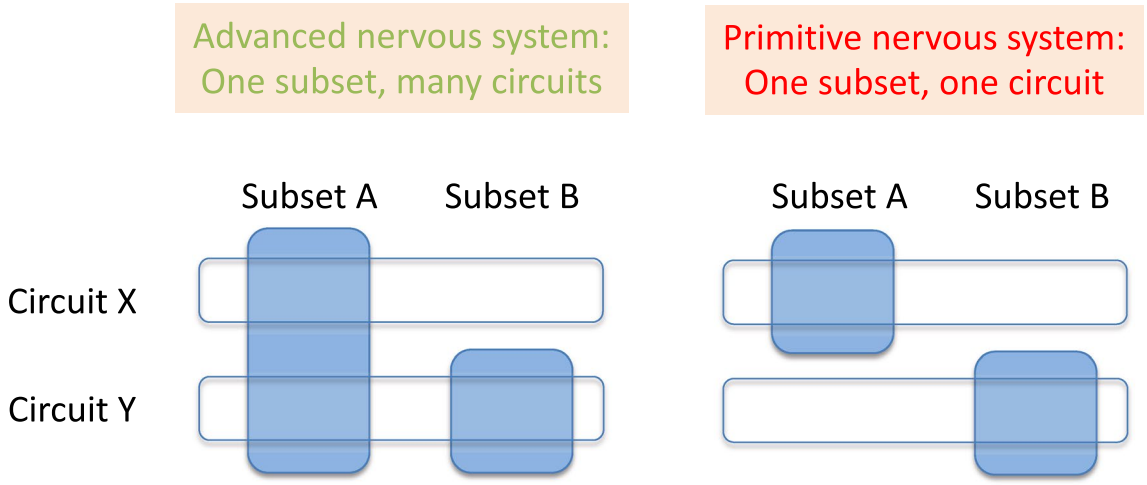

Figure 6. One subset, one circuit in the primitive nervous system. Neuron subset is a molecularly defined group of neurons expressing a common marker gene set. A neuron circuit is a physiologically defined group of neurons, firing simultaneously to function. Usually, a neuron subset harbors multiple neuron circuits in an advanced nervous system while a neuron subset harbors a single neuron circuit for their motor function in *Hydra*.

They named the five coactive circuits CB, STN, RP1, RP2, and Others[19]. However, the molecular identities of these circuits remain unknown.

In this study, we characterized subset-specific neuronal activity to reveal the relationship between functionally identified circuits and molecularly identified subsets. These two are not always identical. We found that each one of the two peptidergic neuron subsets (one expressing *Hym-176B* in the body column (ec1A) and the other expressing *Hym-176A/C* in the peduncle (ec5)) is a coactive motor circuit because the simultaneous excitations of almost all neurons in each subset were followed by longitudinal contractions (Figs. 1, 2, Movies 6–9). This finding demonstrates that a subset consists of a single circuit in *Hydra* (Fig. 6). In contrast, multiple circuits usually share a molecularly defined neuron subset in the bilaterian nervous system[20,21]. Therefore, we propose here that this notion of "one subset, one circuit" is a characteristic feature of the nervous system in *Hydra*.

The circuit CB is the only circuit that Dupre and Yuste identified to be correlated with the longitudinal contraction. The circuit is distributed throughout the whole body except in the tentacle and the basal disk[19]. Their findings on the circuit CB appear to correspond to the two motor circuits that we identified in this study, even though the CB is one single coactive circuit. This may be because the two motor circuits are closely associated with each other temporally. We found that procaine is useful to distinguish the two motor circuits, demonstrating that they are indeed two circuits that are synchronously regulated (Figs. 3, 4). This inter-circuit synchronicity was broken at the onset of contraction burst to exert region-specific motor function (Fig. 4A,C). Alternatively, even with synchronous firing, subsequent contractions were not always synchronized between the circuits due to a physical restriction that prevented simultaneous contraction of the body and the foot (Fig. 4A). These findings demonstrate that the two circuits function independently as region-specific motor circuits. Therefore, we expand the notion mentioned above to the following upgraded notion: "one subset, one circuit, one function".

The coordinated regulation of the region-specific motor circuits may be required to build a more complex behavior, such as somersaulting in *Hydra*[22], in which several simple behavioral units are sequentially executed. Standing animals first attach to the floor with their tentacles (step 1), detach the foot from the floor (step 2), contract the body column to find a new place (step 3), and finally attach the foot to a new place (step 4). The initial foot-specific contraction we observed at the onset of contraction burst may reflect the second and third steps of somersaulting (Figs. 3A–D, 4A–D). Responding to light with the circuit in the head and the unidirectional neurotransmission from head to foot (Fig. 5) implies how light may be one of the triggers for this complex movement.

Nerve-free polyps contract following mechanical stimulation demonstrating that nerve cells are not required to finish longitudinal contraction but required to initiate spontaneous contractions[23]. This may imply that the two Hym-176-related circuits found here are just motor circuits rather than the general motor neurons that finally finish contraction at the neuromuscular junction. However, synaptic contacts of RFa-expressing neurons to the myoneme of epitheliomuscular cells in the peduncle are demonstrated by Koizumi[24]. Besides, RFa and Hym-176 are co-expressed in the peduncle neurons[12]. Thus, the *Hym176A/C/D*-expressing neuron subset in the peduncle is more likely to be a motor neuron.

Finally, it may require more supporting evidence and exhaustive comparisons between different species of cnidarians to demonstrate that this simple feature found here in *Hydra*, "one subset, one circuit, one function" represents an ancestral trait of the nervous system in the last common ancestor between Bilateria and Cnidaria. The wide conservation of neural genes between them usually implies that this simple feature in *Hydra* has been evolved not by loosing the unnecessary neural genes in the last common ancestor but by developing them differently from bilaterians. However, it may also be possible that the nervous system in the common ancestor has

long been no need to change during its evolution to the current nervous system in *Hydra*, because it has been sufficient for *Hydra* to survive until the present day.

In summary, we demonstrated that a molecularly defined peptidergic neuron subset serves as a single coactive motor circuit in the manner of "one subset, one circuit, one function." This would contribute to understand fundamental traits in nervous systems and underlying mechanisms to construct more complex behaviors by assembling functional subsets as behavioral units.

Methods

Ethical approval and animal management. All experiments in this study were designed according to ARRIVE guidelines and conducted following the institutional guideline with the approval of the Institutional Biosafety and Bioethics Committee under the identification number 17IBEC13.

Animals and culture. The transgenic strain AEP of *Hydra vulgaris* was used in all experiments, which were raised and cultured as described below or previously[14,25].

Transgenic reporter lines. Transgenic *Hydra* was generated using a modified method derived from Wittlieb et al.[26] as described previously[14]. Briefly, we replaced GFP in the previously reported expression vectors (Hym-176A::GFP; Acc# LC426372, Hym-176B::GFP; Acc# LC426373, Hym-176C::GFP; Acc# LC426374, Hym-176D::GFP; Acc# LC426375) with the calcium indicator, GCaMP6s (mGCaMP/#40753, Addgene or hGCaMP/codon-optimized, DNA2.0), so that it could be expressed in the neuron subsets expressing each one of the *Hym-176* gene paralogs (*Hym-176A, B, C,* and *D*). The 1- to the 2-cell stage of embryos were microinjected with the vectors. The hatched F0 polyps were screened to select the GCaMP positive polyps, which were then mated to each other or wild AEP to obtain F1 transgenic lines. The transgenic lines, Hym-176B::mGCaMP and Hym-176C::hGCaMP were F1. The transgenic lines, Hym-176A::hGCaMP and Hym-176D::hGCaMP were F0. The double transgenic line (Hym-176B::GCaMP × Hym-176C::GCaMP) were obtained by crossing F1 polyps of Hym-176B::mGCaMP and Hym-176C::hGCaMP. The operative chimera of Hym-176B::mGCaMP and Hym-176A::hGCaMP (Hym-176B::GCaMP + Hym-176A::GCaMP) was made by grafting the upper half of the Hym-176B::mGCaMP line and the lower half of the Hym-176A::hGCaMP line.

Signal detection and quantitative analysis of excitation and longitudinal contraction. Transgenic animals were sandwiched between two slide glasses with a spacer (0.1 mm thick). The GCaMP signals were detected under the fluorescent dissection microscope (SMZ25, Nikon, Japan) equipped with epi-fluorescence attachments and a CMOS camera (ORCA-Flash4.0 v2, Hamahoto, Japan). Neuron firings visualized by GCaMP were recorded at the speed of 30 ms/frame and tracked frame by frame using the Fiji[27] plugin, TrackMate[28] with its default setting (LoG detector; msb: 15–50, threshold: 0.01–4, and Simple LAP tracker). We manually edited the automated tracking results afterward. The tracking data (intensity and position of each neuron at each frame) were analyzed by R[29] and visualized by its graphic package, ggplot2[30]. The relative intensity was calculated by normalizing the total intensity with min–max feature scaling. The longitudinal contraction was evaluated as the change in the distance between two designated neurons through all frames, usually the uppermost and the lowermost neuron in each neuron subset. The distance was also normalized by min–max feature scaling. The second-order difference of the normalized distance was used to determine the start of contraction at its local minimum. Cross-correlation was calculated with function ccf in R. To compare the firing timing between body and foot circuits (Fig. 4B,D,F,H) or with and without attenuation of blue light (Fig. 5E), we carried out a two-sided Student's t-test using the R package, ggsignif[31]. Boxplot elements are defined as follows: center line, median; cross mark, mean; box limits, the first and third quartiles (the 25th and 75th percentiles); whiskers, 1.5 × interquartile range; points, outliers (data beyond the end of the whiskers).

Procaine treatment. Animals were soaked in 1% procaine hydrochloride (P9879, Sigma-Aldrich) in a culture medium. The voluntary longitudinal contraction was stopped after a few minutes while the voluntary excitation was intact. The inter-circuit phase shift of excitation was first observed. Then, the intra-circuit phase shift was observed with prolonged incubation. This effect of procaine was reversible because animals contracted once again in the absence of procaine.

Light-sensitivity test. Hym-176B::GCaMP transgenic animals without buds were first exposed to visible light for 1 min under a microscope to remove overly sensitive animals. The animals that did not contract in response to visible light were subsequently exposed to the blue excitation light, with or without a black filter, to attenuate the intensity by 75%. We measured the time when the light-sensitive cell population started to glow under a microscope with × 30 magnification. Since it usually took more than 2 min for the filtered blue light to trigger excitation, we removed the filter after 1 min exposure. Thus, for the filtered group, if the exposure time before excitation was more than 1 min, the filter was removed after 1 min, and the population was thus exposed without the filter. Three independent experiments were conducted (n = 22 for exp_1 and 2, and n = 14 for exp_3). Statistical significance of the difference between the average time to the beginning of excitation with and without a dark filter was evaluated using a two-sided Student's t-test with the R package, ggsignif[31].

Received: 22 November 2020; Accepted: 23 April 2021
Published online: 24 May 2021

References

1. Dunn, C. W. *et al.* Broad phylogenomic sampling improves resolution of the animal tree of life. *Nature* **452**, 745–749. https://doi.org/10.1038/nature06614 (2008).
2. Ryan, J. F. *et al.* The genome of the ctenophore *Mnemiopsis leidyi* and its implications for cell type evolution. *Science* **342**, 1242592–1242592. https://doi.org/10.1126/science.1242592 (2013).
3. Feuda, R. *et al.* Improved modeling of compositional heterogeneity supports sponges as sister to all other animals. *Curr. Biol.* **27**, 3864-3870.e3864. https://doi.org/10.1016/j.cub.2017.11.008 (2017).
4. Pisani, D. *et al.* Genomic data do not support comb jellies as the sister group to all other animals. *Proc. Natl. Acad. Sci. U.S.A.* **112**, 15402–15407. https://doi.org/10.1073/pnas.1518127112 (2015).
5. Moroz, L. L. *et al.* The ctenophore genome and the evolutionary origins of neural systems. *Nature* **510**, 109–114. https://doi.org/10.1038/nature13400 (2014).
6. Watanabe, H., Fujisawa, T. & Holstein, T. W. Cnidarians and the evolutionary origin of the nervous system. *Dev. Growth Differ.* **51**, 167–183. https://doi.org/10.1111/j.1440-169X.2009.01103.x (2009).
7. Leviev, I., Williamson, M. & Grimmelikhuijzen, C. J. P. Molecular cloning of a preprohormone from *Hydra magnipapillata* containing multiple copies of hydra-LWamide (Leu-Trp-NH2) neuropeptides: Evidence for processing at ser and asn residues. *J. Neurochem.* **68**, 1319–1325. https://doi.org/10.1046/j.1471-4159.1997.68031319.x (1997).
8. Takahashi, T. *et al.* A novel neuropeptide, Hym-355, positively regulates neuron differentiation in Hydra. *Development* **127**, 997–1005 (2000).
9. Darmer, D. *et al.* Three different prohormones yield a variety of Hydra-RFamide (Arg-Phe-NH2) neuropeptides in Hydra magnipapillata. *Biochem. J.* **332**, 403–412 (1998).
10. Yum, S., Takahashi, T., Hatta, M. & Fujisawa, T. The structure and expression of a preprohormone of a neuropeptide, Hym-176 in Hydra magnipapillata. *FEBS Lett.* **439**, 31–34 (1998).
11. Yum, S. *et al.* A novel neuropeptide, Hym-176, induces contraction of the ectodermal muscle in hydra. *Biochem. Biophys. Res. Commun.* **248**, 584–590 (1998).
12. Hansen, G. N., Williamson, M. & Grimmelikhuijzen, C. J. P. Two-color double-labeling in situ hybridization of whole-mount Hydra using RNA probes for five different Hydra neuropeptide preprohormones: Evidence for colocalization. *Cell Tissue Res.* **301**, 245–253 (2000).
13. Hansen, G. N., Williamson, M. & Grimmelikhuijzen, C. J. P. A new case of neuropeptide coexpression (RGamide and LWamides) in Hydra, found by whole-mount, two-color double-labeling in situ hybridization. *Cell Tissue Res.* **308**, 157–165 (2002).
14. Noro, Y. *et al.* Regionalized nervous system in Hydra and the mechanism of its development. *Gene Expr. Patterns* **31**, 42–59. https://doi.org/10.1016/j.gep.2019.01.003 (2019).
15. Siebert, S. *et al.* Stem cell differentiation trajectories in Hydra resolved at single-cell resolution. *Science* **365**, 9314. https://doi.org/10.1126/science.aav9314 (2019).
16. Chen, T.-W. *et al.* Ultrasensitive fluorescent proteins for imaging neuronal activity. *Nature* **499**, 295. https://doi.org/10.1038/nature12354 (2013).
17. Josephson, R. K. Spontaneous electrical activity in a hydroid polyp. *Comp. Biochem. Physiol.* **5**, 45–58. https://doi.org/10.1016/0010-406X(62)90140-8 (1962).
18. Passano, L. M. & McCullough, C. B. The light response and the rhythmic potentials of Hydra. *Proc. Natl. Acad. Sci.* **48**, 1376–1382. https://doi.org/10.1073/pnas.48.8.1376 (1962).
19. Dupre, C. & Yuste, R. Non-overlapping neural networks in *Hydra vulgaris*. *Curr. Biol.* **27**, 1085–1097. https://doi.org/10.1016/j.cub.2017.02.049 (2017).
20. Zeisel, A. *et al.* Cell types in the mouse cortex and hippocampus revealed by single-cell RNA-seq. *Science* **347**, 1138. https://doi.org/10.1126/science.aaa1934 (2015).
21. Daigle, T. L. *et al.* A suite of transgenic driver and reporter mouse lines with enhanced brain-cell-type targeting and functionality. *Cell* **174**, 465–480. https://doi.org/10.1016/j.cell.2018.06.035 (2018).
22. Trembley, A., Pronk, C., Schley, J. V. D. & Lyonet, P. *Mémoires Pour Servir à l'histoire d'un Genre de polypes d'eau douce, à bras en forme de cornes* (Chez Jean & Herman Verbeek, 1944).
23. Campbell, R. D. Elimination by Hydra interstitial and nerve cells by means of colchicine. *J. Cell Sci.* **21**, 1–13 (1976).
24. Koizumi, O., Wilson, J. D., Grimmelikhuijzen, C. J. & Westfall, J. A. Ultrastructural localization of RFamide-like peptides in neuronal dense-cored vesicles in the peduncle of Hydra. *J. Exp. Zool.* **249**, 17–22. https://doi.org/10.1002/jez.1402490105 (1989).
25. Sugiyama, T. & Fujisawa, T. Genetic analysis of developmental mechanisms in Hydra I. Sexual reproduction of *Hydra magnipapillata* and isolation of mutants. *Dev. Growth Differ.* **19**, 187–200. https://doi.org/10.1111/j.1440-169X.1977.00187.x (1977).
26. Wittlieb, J., Khalturin, K., Lohmann, J. U., Anton-Erxleben, F. & Bosch, T. C. G. From the cover: Transgenic Hydra allow in vivo tracking of individual stem cells during morphogenesis. *PNAS* **103**, 6208–6211. https://doi.org/10.1073/pnas.0510163103 (2006).
27. Schindelin, J. *et al.* Fiji: An open-source platform for biological-image analysis. *Nat. Methods* **9**, 676. https://doi.org/10.1038/nmeth.2019 (2012).
28. Tinevez, J.-Y. *et al.* TrackMate: An open and extensible platform for single-particle tracking. *Methods* **115**, 80–90. https://doi.org/10.1016/j.ymeth.2016.09.016 (2017).
29. Team, R. C. R: A Language and Environment for Statistical Computing. *R Foundation for Statistical Computing* (2018).
30. Wickham, H. *ggplot2: Elegant Graphics for Data Analysis* (Springer, 2016).
31. Ahlmann-Eltze, C. ggsignif: Significance Brackets for 'ggplot2' (2019).

Acknowledgements

This work was supported through funding from King Abdullah University of Science and Technology (KAUST) under award numbers BAS/1/1059/01/01 and URF/1/1976/03/01.

Author contributions

Y.N., H.S. and T.G. designed the research. Y.N. performed most of the experiments. H.S. raised and maintained transgenic lines together with Y.N. K.M. contributed a lot to the computational works done by Y.N. All the authors wrote the manuscript.

Competing interests

The authors declare no competing interests.

Additional information

Supplementary Information The online version contains supplementary material available at https://doi.org/10.1038/s41598-021-89325-x.

Correspondence and requests for materials should be addressed to T.G.

Reprints and permissions information is available at www.nature.com/reprints.

Publisher's note Springer Nature remains neutral with regard to jurisdictional claims in published maps and institutional affiliations.